Proceedings of the 11th
KACC, October 1996

INDUCTION MOTORS WITH ELECTROSTATIC SUSPENSION

°Jong Up Jeon*, Shao Jü Woo*, and Toshiro Higuchi*,**

*Kanagawa Academy of Science and Technology, East Block 405, KSP, 3-2-1 Sakado, Takatsu-ku, Kawasaki 213, JAPAN
Tel: +81-44-819-2093; Fax: +81-44-819-2095; E-mail: jeon%naeba@intellect.pe.u-tokyo.ac.jp

**Dept. of Precision Machinery Eng., The University of Tokyo, 7-3-1 Hongo, Bunkyo-ku, Tokyo 113, JAPAN
Tel:+81-3-3812-2111 ext. 6449; Fax:+81-3-5800-6968; E-mail: higuchi@intellect.pe.u-tokyo.ac.jp

Abstract This paper studies electrostatically suspended induction motors (ESIM). The ESIM possesses the rotating ability of an ordinary electrostatic induction motor, in addition to providing contactless support by electrostatic suspension. To accomplish these two functions, a feedback control strategy and the operating principle of an ordinary electrostatic induction motor are used. The stator possesses electrodes which exert the electrostatic forces to the rotor and are divided into a part responsible for suspension and one for rotation. Two rotor types are utilized: a polished glass disk without any surface treatment, and a polished glass disk covered with a thin layer of conductive material (ITO layer) on only one side. In this paper, the principle of the ESIM is described, followed by stator electrode design, experimental apparatus, control strategy for stable suspension. Experimental results show that the glass disk has been rotated with a speed of approximately 70 rpm while being suspended stably at a gap length of 0.3 mm.

Keywords Electrostatic Force, Electrostatic Suspension, LCD, Electrostatic Motor, Glass Disk Suspension, Glass Disk Rotation

1. INTRODUCTION

In the manufacturing process of liquid crystal display (LCD) devices, the handling of a glass panel by mechanical contact is becoming more critical since its thickness/surfacial area ratio is becoming smaller. Moreover, the physical contact with a glass plate will contaminate the surface of the glass plate and also will generate the particles. Thus, glass plate handling systems without any physical contact are indispensable.

To implement the function of contactless support and actuating function, magnetically suspended stepping actuators have already been studied [1]. However, these actuators can not handle glass plates directly since magnetic forces can not exert forces on them. Therefore, in order to manipulate a non-ferromagnetic object such as a glass plate, additional devices to support it are needed, which leads to direct mechanical contact resulting in surface contaminations of the glass plate and particle generation. Electrostatic suspension has the potential to remedy the above problem. Various types of materials such as conductive materials, semiconductors and dielectric materials can be suspended directly by electrostatic forces. A silicon wafer has already been suspended by actively controlling electrostatic forces exerted on it [2].

Several electrostatic induction motors whose dimensions and structures are analogous to conventional electromagnetic motors have been developed [3-4]. However, these types of motors do not possess the function of contactless support of the rotor since the rotor is supported by bushing. A multi-layered electrostatic film actuator has also been developed to realize high force/weight ratio actuators applicable for large scale machines [5]. In this actuator, the slider films slide in/out between the stator films and thus friction between these films comes into existence. Therefore, a function of suspension has to be incorporated in addition to an actuating function in order to implement contactless and friction-free handling devices for non-ferromagnetic materials such as glass.

This paper reports about the successful suspension and rotation of a glass disk using electrostatic forces. The actuator possessing these two functions is named as electrostatically suspended induction motor (ESIM).

2. PRINCIPLE OF ELECTROSTATICALLY SUSPENDED INDUCTION MOTORS (ESIM)

The ESIM is an electrostatic induction motor where the rotor is supported contactless using electrostatic forces. By locating the stator electrodes above the rotor, attractive electrostatic forces can be exerted on the rotor. However, if d.c. voltages are applied to the stator electrodes, the rotor movements along the vertical, pitching and rolling directions will exhibit unstable behavior. Therefore, in order to stabilize the rotor motions, active control of the electrostatic forces is performed in such a way that the voltages applied to the stator electrodes are controlled based on the rotor position/attitude [2].

With respect to the motion in the plane of the rotor, passive stabilization is guaranteed through the existence of a restriction force. This restriction force arises from a relative lateral translation of the rotor with respect to the stator electrodes [6]. Therefore, active control of the rotor movements along vertical, pitching and rolling direction is sufficient to implement a stable rotor support by electrostatic forces.

The operating principle of rotation in ESIM, like ordinary electrostatic induction motors, is based on the fact that a rotor made of

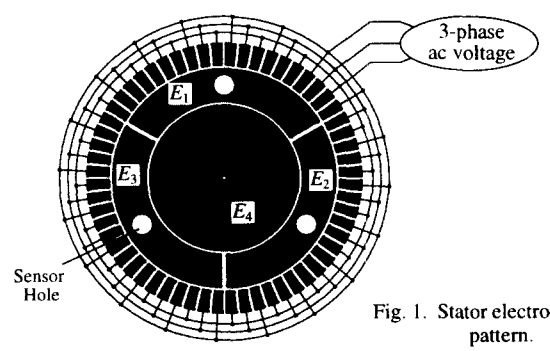

Fig. 1. Stator electrode pattern.

a material which is slightly electrically conducting (a "poor insulator") is subjected to a torque when placed in a rotating electric field [3]. The explanation for this lies in the fact that the high resistivity causes the induced charges on the rotor surface to lag behind the rotating field. As a consequence, a torque will be exerted by the rotating field on those charges and hence on the rotor. In ESIM, the rotating electric field is generated by supplying a.c. voltages to a number of teeth formed on the stator. As rotor material, glass is employed which is slightly conductive.

3. EXPERIMENTAL WORK

3.1 Experimental System

3.1.1 Stator Electrode Design

Fig. 1 depicts the electrode pattern of the stator. The stator electrodes comprise two functionally distinct parts. The central area is used for stable suspension of the rotor and the peripheral area is used for the generation of a torque to rotate it. The suspension area is subdivided into four sections (denoted as E_j, where j=1,2,3,4), each of which act as independent actuators of force on the rotor. Among them, the outer three electrodes E_1, E_2 and E_3, which together form a ring, have the same shape and area. The area of electrode E_4 is three times that of E_1. To measure the gap length between each electrode E_i (i=1,2,3) and the rotor, each individual electrode E_i is supplied with a fiber optical sensor.

The outer region of the stator electrodes consists of a number of teeth with an uniform tooth pitch along the circumference of the stator electrodes. Each tooth is connected to form three phases.

3.1.2 Experimental Apparatus

Fig. 2 shows the schematic diagram of the experimental apparatus. The stator electrodes are etched from a 35 μm thick copper layer on a glass-epoxy base. Electrodes #1, #2 and #3 have the same area of 7.6 cm^2. The teeth for rotation have a pitch of 6 degrees and a tooth length of 8 mm. The gaps between the teeth are 1 mm. Fig. 3 depicts a photograph of the stator. Two types of rotors were utilized: a polished soda-lime glass disk without any surface treatment, and a polished glass disk covered on only one side with a thin layer of conductive material (ITO layer). Both of the glass disks have a diameter of 100 mm, a thickness of 0.7 mm and a mass of about 13.5 g. The surface resistivity and the volume resistivity of the glass disk without any surface treatment were measured to be approximately 10^{14} Ω and 10^{13} Ω·cm, respectively, for an air humidity of 50 %RH and temperature of 25 °C, while the surface resistivity of the ITO layered disk was about 10^6 Ω. In case of the ITO layered glass disk, the side of the disk without ITO layer should be positioned to face the stator electrodes. Utilization of an ITO layer contributes to an improvement of the suspension and rotational performance, which was verified experimentally. By adjusting the heights of the upper and lower micropositioning screws, the stator

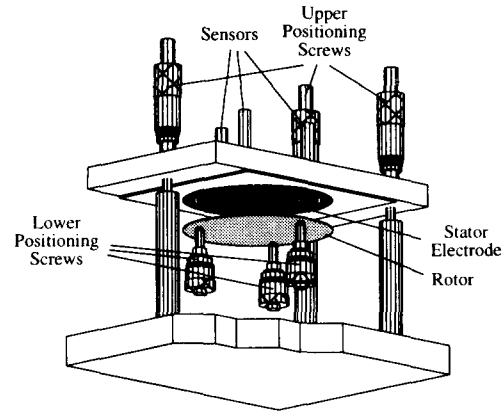

Fig. 2. Schematic diagram of experimental apparatus.

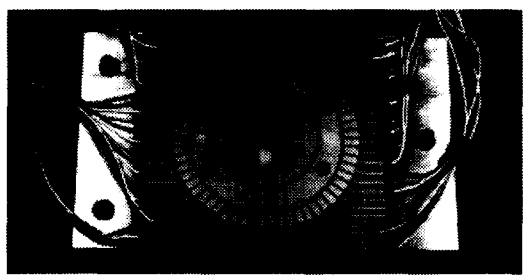

Fig. 3. Photograph of stator.

electrode is leveled and the initial gap length is set.

3.1.3 Control Strategy

To implement a stable suspension, voltages applied to the electrodes-for-suspension E_j, where j=1~4, are actively controlled. In this paper, the method to stabilize the rotor movement will be described briefly. For a more detailed description, reference is made to [7]. Fig. 4 shows the block diagram of the control system for suspension. The principle of control is similar to that of electromagnetic levitation system. The three gap lengths d_{si}^*, where i=1, 2, 3, between the stator electrodes E_i and the rotor at the sensor positions are measured by using three gap sensors. From these measured gap lengths d_{si}^*, the gap deviations d_{si} from the reference gap lengths d_{s0i} are determined and then transformed to the rotor position/attitude error signals; vertical movement z, pitch angle θ and roll angle ψ. These error signals α, where α=z, θ, ψ, are fed back to a PID compensator which determines the control voltages V_α with respect to the rotor movement in each degree of freedom. The control voltages V_α are transformed to the control voltages V_i by a precompensation matrix and then combined with the bias voltages V_{0i} to produce the total voltages V_i^* (i=1, 2, 3) which are to be applied to the electrodes-for-suspension E_i and have positive polarities. From the total voltages V_i^* and the capacitances C_j^* between the elec-

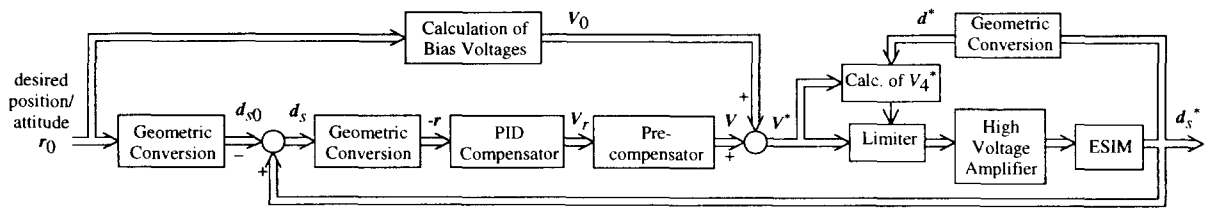

Fig. 4. Block diagram of control system for suspension.

(Definition of variables: r_0=(α_0), r=(α), d_s^*=(d_{si}^*), d_{s0}=(d_{s0i}), d_s=(d_{si}), d^*=(d_j^*), V_r=($V_{r\alpha}$), V_i^*=(V_i^*), V_{0i}=(V_{0i}), V_i=(V_i), where α=z, θ, ψ, i=1~3 and j=1~4.)

trodes E_j and the rotor, the total voltage V_4^* applied to the electrode E_4 can be obtained as follows

$$V_4^* = -\frac{\sum_{k=1}^{3} C_k^* V_k^*}{C_4^*}$$

where $C_j^*=(\varepsilon A_j)/d_j^*$, ε denotes the permittivity, A_j denotes the area of the electrode E_j, and d_j^* denotes the gap length between the electrode E_j and the rotor at the geometrical center of the electrode. Note that the polarity of the voltages applied to electrode E_1, E_2 and E_3 is positive while that of the voltage applied to the electrode E_4 is negative. This generates a potential difference between the electrodes and the rotor and consequently electrostatic forces can be exerted on the rotor. After going through four limiter circuits, the four voltage signals are sent to four high voltage amplifiers and supplied to the four electrodes-for-suspension E_j. Note that a limitation is imposed on the voltages for suspension to prevent electric discharge which is caused by the breakdown of the electric field. The high voltage amplifiers have an amplification ratio of 1000.

To generate a rotating electric field and consequently a rotational torque on the rotor, three-phase a.c. voltages differing in phase by 120° are supplied to the three phases of the electrodes-for-rotation.

3.2 Experimental Results and Discussion

Prior to rotation, suspension experiments were carried out with the polished glass disk having no surface treatment in an atmospheric environment. The applied proportional, derivative and integral gains for the vertical movement of the rotor were respectively 10^5 kV/m, 90 kV·s/m and 10^6 kV/(m·s), and those for pitching and rolling were 60 kV/rad, 0.06 kV·s/rad and 10^3 kV/(rad·s), respectively. A bias voltage of $\pm$0.78 kV was supplied to the electrodes-for-suspension. The initial and reference gap length were 350 μm and 300 μm, respectively. Fig. 5 shows the recorded gap length and voltage variations after the PID compensator was switched on. It shows that a period of time of approximately 40 seconds was needed for the glass disk to actually reach a state of suspension. Note that since glass is a material having a high resistivity, a certain period of time is needed to accumulate sufficient induced charges on the glass surface facing the electrodes-for-suspension for picking up the rotor. This period of time is strongly dependent on the environmental humidity. The data shown in Fig. 5 was recorded under an air humidity of 50 %RH. From our experiments, it was observed that the period of time needed to achieve a stable suspension varied from 1 seconds to 2 minutes for a humidity variation from 70 %RH to 30 %RH. Fig. 5 also shows that during the state of stable suspension, the actively controlled voltages are slowly decreasing. A physical explanation for this drift phenomenon is that the charge built-up on the glass surface had not yet reached a steady state and indicates that the process of charge accumulation was progressing continuously during suspension. The voltages after 3 minutes from the control start were respectively 0.8 kV, 0.8 kV, 0.78 kV and -0.8 kV. Fig. 6 is a photograph of the glass disk under stable suspension.

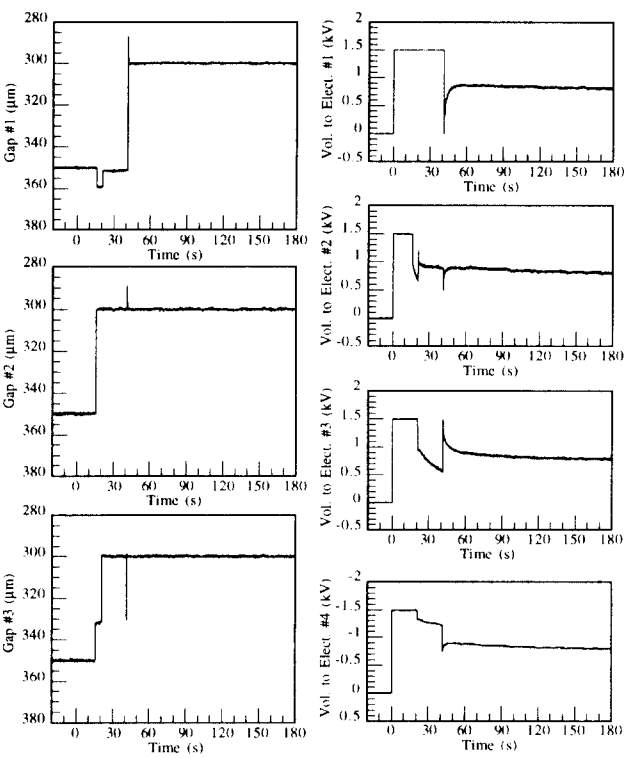

Fig. 5. Gap and voltage variations during suspension process. (Rotor is polished glass disk without any surface treatment.)

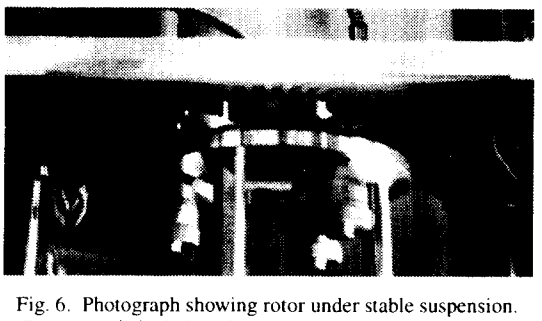

Fig. 6. Photograph showing rotor under stable suspension. (Rotor is polished glass disk without any surface treatment.)

Rotation was enabled by supplying three-phase a.c. voltages of 1 kV p-p to the electrodes-for-rotation after a stable suspension was reached. We have succeeded in rotating the glass disk with a maximum speed of 70 rpm. The main factor restricting the maximum speed is not the rotational torque but the passive lateral restriction force. When the rotor speed reached above 70 rpm, the motion of the rotor along the lateral direction became unstable due to an insufficiency of the restorative forces. Concerning the maximum acceleration, it was recorded that a time period of 2 seconds was required to raise the speed from 0 rpm to 70 rpm. Fig. 7 shows the gap length and voltage variations at a rotor speed of 60 rpm. The gap fluctuations did not exceed 2 μm p-p while the voltage fluctuations supplied to electrodes #1, #2, #3 and #4 were 0.12 kV, 0.1 kV, 0.1 kV, and 0.02 kV, respectively.

The lateral motion of the glass plate reveals a hysteretic-like characteristic so that in the event of an lateral disturbance, the disk does not return back to its original position even after removing the disturbance. It is known that in case of a rotor consisting of conductive material, the lateral restorative forces are generated due to the edge effect. However, in case that the rotor consisted of highly resistive or dielectric material like glass, it was observed that these edge effects are small and the lateral restriction forces are mainly generated in the vicinity of the boundaries of the electrodes having a potential difference. This results in the hysteretic-like characteristic of the lateral motion of the rotor. In our experiments, it was not so easy to obtain a repeatable rotational performance, such as the

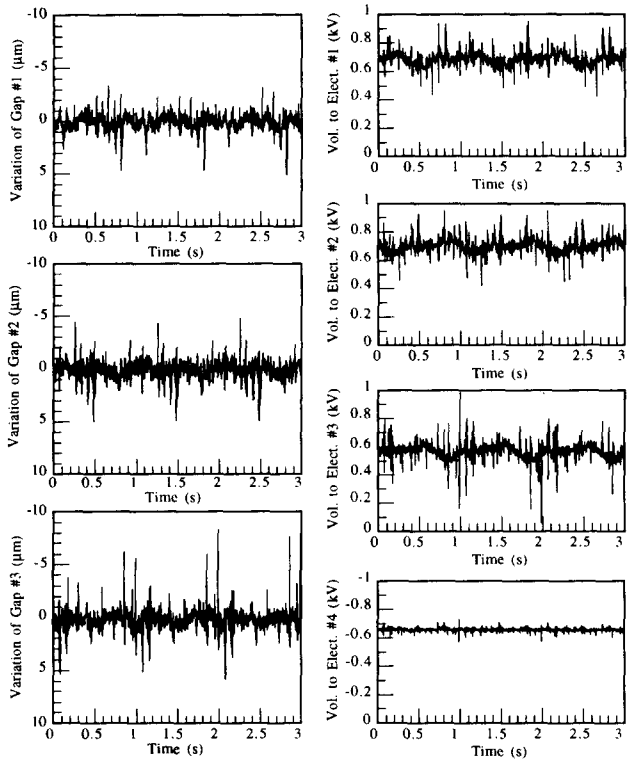

Fig. 7. Gap and voltage variations during rotation.
(Rotor is polished glass disk without any surface treatment.)

attainable maximum speed or lateral vibration, because of the hysteretic-like characteristic.

Next, the suspension and rotation experiments were carried out with the ITO layered glass disk. The control gains used were the same as those in case of the glass plate without any surface treatment. A bias voltage of ± 0.67 kV was utilized. Fig. 8 shows the variations of the gap lengths and voltages after the PID compensator was switched on. It shows that the glass disk was pulled up immediately after switching on the PID compensator. This is due to the ITO layer on the lower surface of the glass plate.

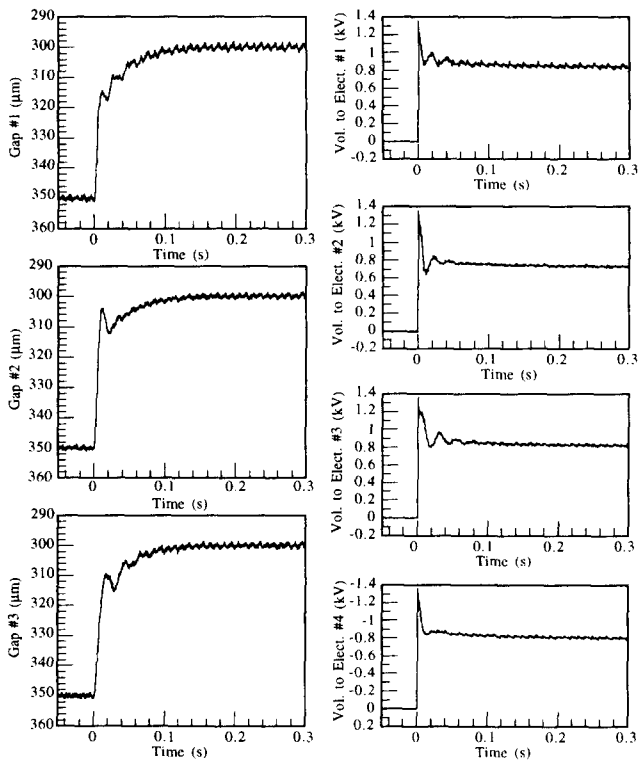

Fig. 8. Gap and voltage variations during suspension process.
(Rotor is made of ITO layered glass.)

Rotation experiments were conducted by supplying three-phase a.c. voltages of 1 kV p-p to the electrodes-for-rotation. The glass disk was rotated successfully with a maximum speed of approximately 60 rpm. As in case of the glass plate without any surface treatment, the maximum attainable rotor speed was limited by the lateral restriction forces. However, owing to the ITO layer, the lateral motion of the disk did not exhibit any hysteretic-like characteristic and therefore a repeatable rotational performance could be obtained.

The ESIM is an asynchronous motor. Nevertheless, it was observed that the rotor speed was synchronous to the frequency of the supplied voltage. The reason for this is that the torque produced by ESIM is large enough to overcome the external torques which is caused only by air friction since the rotor is suspended contactless.

4. CONCLUSIONS

Electrostatically suspended induction motor (ESIM), which is a rotary actuator with a function of contactless rotor support by electrostatic forces, was described in this paper. ESIM features stator electrodes which are subdivided into a part responsible for suspension and one for rotation. To implement a stable suspension, the voltages supplied to the electrodes-for-suspension are actively controlled on the basis of the rotor position/attitude. Three-phase a.c. voltages are supplied to the electrodes-for-rotation to generate a rotating electric field on the surface of the rotor. As a rotor, a polished glass disk without any surface treatment and a one-side ITO layered glass disk were used. The glass disks have been suspended successfully at a gap length of 300 μm and rotated with a rotational speed of approximately 70 rpm during suspension. The gap fluctuations were found to be no greater than 2 μm during rotation. The proposed actuator is expected to be widely used in industrial applications as a contactless-supporting and actuating device for dielectric materials like glass.

REFERENCES

[1] T. Higuchi, A. Horikoshi and T. Komori, "Development of an Actuator for Super Clean Rooms and Ultra High Vacua", *Proc. 2nd Int. Symp. Magnetic Bearings*, Tokyo, Japan, pp.115-122, July 1990.

[2] J. Jin, T. Higuchi and M. Kanemoto, "Electrostatic Silicon Wafer Suspension", *Proc. 4th Int. Symp. Magnetic Bearings*, ETH Zürich, Switzerland, pp. 343-348, August 1994.

[3] B. Bollée, "Electrostatic Motors", *Philips Technical Review*, Vol. 30, No. 6/7, pp. 178-194, 1969.

[4] S. D. Choi and D. A. Dunn, "A Surface-Charge Induction Motor", *Proc. IEEE*, Vol. 59, No. 5, pp. 737-748, 1971.

[5] S. Egawa and T. Higuchi "Multi-Layered Electrostatic Film Actuator", *Proc. 1990 IEEE Workshop on Micro Electro Mechanical Systems*, Napa Valley, CA, pp. 166-171, 1990.

[6] S. J. Woo, J. U. Jeon, T. Higuchi and J. Jin, "Electrostatic Force Analysis of Electrostatic Levitation System", *Proc. 34th SICE Annual Conf.*, International Session, Hokkaido, Japan, pp. 1347-1352, July 1995.

[7] J. U. Jeon, J. Jin and T. Higuchi, "Rotary Actuators with Electrostatic Suspension", *Proc. 5th Int. Symp. Magnetic Bearings*, Kanazawa, Japan, pp. 411-418, August 1996.